Acta Crystallographica Section C
Crystal Structure Communications
ISSN 0108-2701

$[CuCl_3(H_2O)]^-$ complexes aggregated to form hydrate columns in methyl-substituted pyridinium or piperidinium salts

Sowjanya Nalla and Marcus R. Bond*

Department of Chemistry, Southeast Missouri State University, Cape Girardeau, MO 63701, USA
Correspondence e-mail: bond@mbond2.st.semo.edu

Received 3 April 2011
Accepted 7 May 2011
Online 18 May 2011

1,2,3-Trimethylpyridinium aquatrichloridocuprate(II), $(C_8H_{12}N)[CuCl_3(H_2O)]$, (I), 3,4-dimethylpyridinium aquatrichloridocuprate(II), $(C_7H_{10}N)[CuCl_3(H_2O)]$, (II), and 2,3-dimethylpyridinium aquatrichloridocuprate(II), $(C_7H_{10}N)[CuCl_3(H_2O)]$, (III), exhibit the same fundamental structure, with (I) and (II) isomorphous and with the unit-cell constants of (III) similar to the reduced unit-cell constants of (I) and (II). The distorted square-planar $[CuCl_3(H_2O)]^-$ complex [mirror symmetric in (I) and (II)] forms two semicoordinate Cu···Cl bonds to a neighboring complex to produce a dimer with 2/*m* symmetry [only inversion symmetry in (III)]. The semicoordinate Cu···Cl bond length of the dimer shows significant elongation at 295 K compared with that at 100 K, while the coordinate Cu—Cl bond lengths are slightly contracted at 295 K compared with those at 100 K. The inorganic dimers are linked by eight hydrogen bonds to four neighboring dimers to establish a checkerboard network layer in the *ab* plane, with voids between the dimers that accommodate, on both sides, inversion-related organic cation pairs. The organic cations are required by mirror-plane symmetry to be disordered in (I) and (II). The organic cations and $[CuCl_3(H_2O)]^-$ complexes are nearly coplanar and tilted out of the layer plane to establish a hybrid organic–inorganic layer structure parallel to (202) [(11$\bar{2}$) in (III)], with hydrate columns (defined by water molecules) and hydrophobic columns (defined by methyl groups) parallel to each other [and along the 2_1 axes in (I) and (II)]. In 1,1-dimethylpiperidinium aquatrichloridocuprate(II), $(C_7H_{16}N)[CuCl_3(H_2O)]$, (IV), the bulkier organic cation prevents semicoordinate bonding between complexes, which are hydrogen bonded side-to-side in zigzag chains that place water molecules in columns along half of the 2_1 axes.

Comment

In the first major study of $[CuCl_3(H_2O)]^-$ complexes, Manfredini *et al.* (1990) noted that halidocuprate(II) complexes disubstituted by neutral *N*- or *O*-donor ligands are more common than monosubstituted complexes. Compounds containing $[CuCl_3(H_2O)]^-$ complexes are still rare, with only 12 identified in the Cambridge Structural Database (CSD, Version 5.32; Allen, 2002), and a further nine complexes with other *O*-donor ligands, compared with at least 55 compounds containing $CuCl_2L_2$ complexes (where *L* is a neutral *O*-donor ligand). Geometries of known $[CuCl_3(H_2O)]^-$ complexes (and aggregation motifs) are summarized in Table 1, which shows that the coordination environments of the complexes range from square planar to flattened tetrahedral to regular tetrahedral. Meanwhile, a range of aggregation schemes, ranging from stacks of complexes linked by semicoordinate Cu···Cl bonds to hydrogen-bonded chains or ribbons to isolated complexes, is also found. We present here four compounds that contain $[CuCl_3(H_2O)]^-$ complexes aggregated in structural motifs that differ from those found in previously observed structures, while also establishing a persistent $ACuCl_3(H_2O)$ structure type for three of the four compounds.

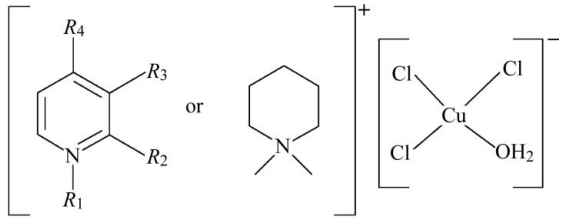

(I) $R_1 = R_2 = R_3 = Me$, $R_4 = H$ (IV)
(II) $R_1 = R_2 = H$, $R_3 = R_4 = Me$
(III) $R_1 = R_4 = H$, $R_2 = R_3 = Me$

The 1,2,3-trimethylpyridinium, (I), 3,4-dimethylpyridinium, (II), and 2,3-dimethylpyridinium, (III), salts of $[CuCl_3(H_2O)]^-$ exhibit the same fundamental structure. Compounds (I) and (II) are isomorphous, crystallizing in the monoclinic space group *C*2/*m*, while (III) crystallizes in the triclinic space group $P\bar{1}$ with cell constants that are similar to the reduced unit-cell constants of (I) and (II) [reduced cell constants of $a = b = 9.0081\ (2)$ Å, $c = 8.4159\ (2)$ Å, $\alpha = \beta = 77.788\ (2)^\circ$ and $\gamma = 61.781\ (2)^\circ$ for (I) at 100 K]. A marked contraction in *a* is observed on cooling from 295 to 100 K in (I) and (II), decreasing by 1.45% in (I) and by 1.12% in (II), in contrast with a slight expansion in *b*. This behavior is also observed in the pseudo-monoclinic cell for (III) [transformation matrix (110/$\bar{1}$10/00$\bar{1}$)], but here the contraction in *a*′ (= [110]) is smaller (0.62%), while *b*′ (= [$\bar{1}$10]) still expands slightly. The structures consist of asymmetrically dibridged dimeric anions that are linked by hydrogen bonding to form a network layer in the *ab* plane, which then stacks alternately along *c* with layers of inversion-related organic cation pairs. The similarity in the *a* and *b* lengths, as well as the (almost) 60° angle between them, in (III) indicates that the approximate orthohexagonal structure of the hydrogen-bonded network layer found in (I) and (II) persists. While not previously observed in $[CuCl_3(H_2O)]^-$ structures, the asymmetrically dibridged dimer is a common motif in $CuCl_2L_2$ compounds, found in 13 of the 55 reported compounds. However, in these cases, the *O*-donor ligands are functionalized organic mol-

 doi:10.1107/S0108270111017306

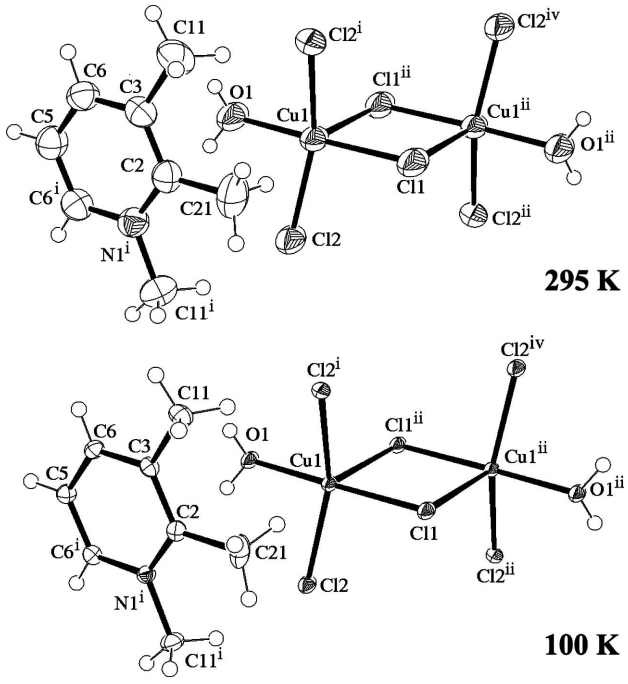

Figure 1
Views of the organic cation and $\{[CuCl_3(H_2O)]_2\}^{2-}$ dimer in (I), at 295 K (top) and 100 K (bottom), showing the atom-labeling scheme. Displacement ellipsoids are drawn at the 50% probability level. The organic cation exhibits mirror-plane-generated twofold disorder. [Symmetry codes: (i) x, $-y$, z; (ii) $-x+1$, y, $-z$; (iv) $-x+1$, $-y$, $-z$.]

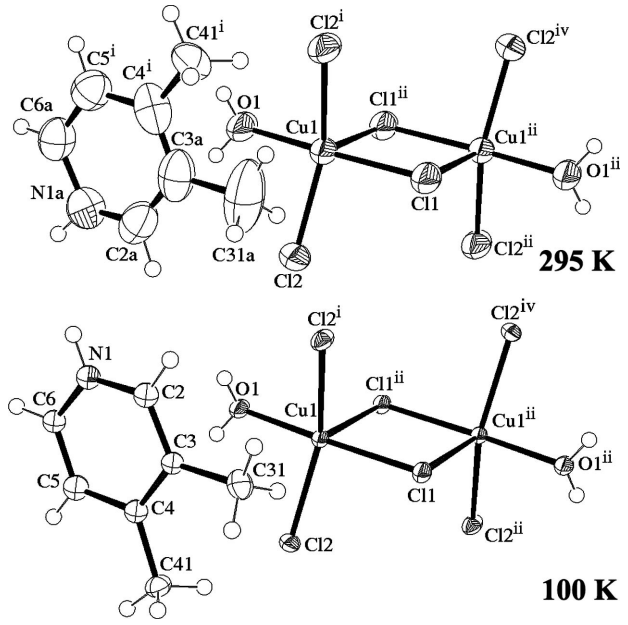

Figure 2
Views of the organic cation and $\{[CuCl_3(H_2O)]_2\}^{2-}$ dimer in (II), at 295 K (top) and 100 K (bottom), showing the atom-labeling scheme. Displacement ellipsoids are drawn at the 50% probability level. The organic cation exhibits mirror-plane-generated twofold disorder. [Symmetry codes: (i) x, $-y$, z; (ii) $-x+1$, y, $-z$; (iv) $-x+1$, $-y$, $-z$.]

ecules that prevent the formation of the hydrogen-bonded network layer structure found in (I)–(III).

The $[CuCl_3(H_2O)]^-$ complex is mirror symmetric in (I) and (II), while the asymmetrically dibridged dimers formed by Cu···Cl semicoordinate bonding have 2/*m* symmetry [inversion symmetry only in (III)]. The *trans* Cl1—Cu1—O1 angle is almost linear for (I) at 100 K but is less linear at 295 K, and more so again in (II) and (III). The *trans* Cl2—Cu1—Cl2^{i} angle [symmetry code: (i) x, $-y$, z; Cl2—Cu1—Cl3 for (III)] is more bent (152–158°), with the most bent angle found for (III), and with the angle becoming less bent at the higher temperature for all. The presence of the semicoordinate Cu1···Cl1^{ii} bond [symmetry code: (ii) $-x+1$, y, $-z$] [Cu1···Cl1^{iii} for (III); symmetry code: (iii) $-x+1$, $-y+2$, $-z$] produces a coordination environment similar to that found by Menon *et al.* (1994) in CSD refcode WETFAC, in which a $[CuCl_3(H_2O)]^-$ complex forms a semicoordinate bond to a lattice chloride, although in WETFAC the *trans* Cl—Cu—O bond is more bent and the *trans* Cl—Cu—Cl bond close to linear. The structural description reported for this complex was 'folded' square-pyramidal, referring to an earlier empirical study of five-coordinate Cu^{II} complexes (Willett, 1985). $CuCl_4(H_2O)^{2-}$ complexes have been reported by Savel'eva *et al.* (1999) (CSD refcode HOWCOL) and Dobrzycki & Wozniak (2008) (COCNEO) that do conform closely to square-pyramidal geometry, but in the former case the complexes are linked by distant semicoordinate bonds to neighboring complexes to form chains in which the true Cu^{II} environment is 4+1+1′. In the latter, the H_2O ligand is axial and semicoordinate, rather than Cl. So these structures offer a poor correlation with those of (I)–(III) and WETFAC.

A more sophisticated analysis of five-coordinate Cu^{II} by Reinen & Astanasov (1989) provides a different interpretation of the folded square-pyramidal geometry. The starting geometry is, instead, trigonal–bipyramidal Cu^{II} that then undergoes a second-order Jahn–Teller distortion to produce a complex with *mm*2 (Schönflies C_{2v}) symmetry, which is intermediate between trigonal–pyramidal and square-pyramidal. This intermediate complex arises from a stretching distortion of the equatorial Cu—Cl bonds (two shorten and one lengthens) and from a bending distortion that increases the angle between the shortened equatorial bonds. The environment around Cu1 in (I)–(III) can thus be described as *mm*2 distorted trigonal–bipyramidal, with atoms Cl1 and O1 the axial ligands and Cl1^{ii}, Cl2 and Cl2^{i} [Cl1^{iii}, Cl2 and Cl3 for (III)] the equatorial ligands. The average equatorial Cu—Cl bond lengths at 100 K of 2.4561 (6) Å in (I), 2.4372 (4) Å in (II) and 2.4457 (12) Å in (III) are not much longer than the average equatorial Cu—Cl bond length in low-temperature $[Cr(NH_3)_6]CuCl_5$ [2.397 (4) Å; Ohba *et al.*, 1995]. The $[M(NH_3)_6]CuCl_5$ structures (*M* is Co or Cr) provided archetypal examples of the *mm*2 distorted trigonal–bipyramidal complex, after the compressed trigonal–bipyramidal complexes at room temperature were found to transform to disordered *mm*2 distorted complexes at lower temperature (Reinen & Friebel, 1984). The elongated equatorial Cu—Cl bond is >0.2 Å longer in (I)–(III) than in $[Cr(NH_3)_6]CuCl_5$ [2.554 (4) Å], so the Cu^{II} complexes in (I)–(III) are not as fully five-coordinate. As a result, the *trans* Cl—Cu—Cl angle (containing the shorter equatorial bonds) is significantly wider

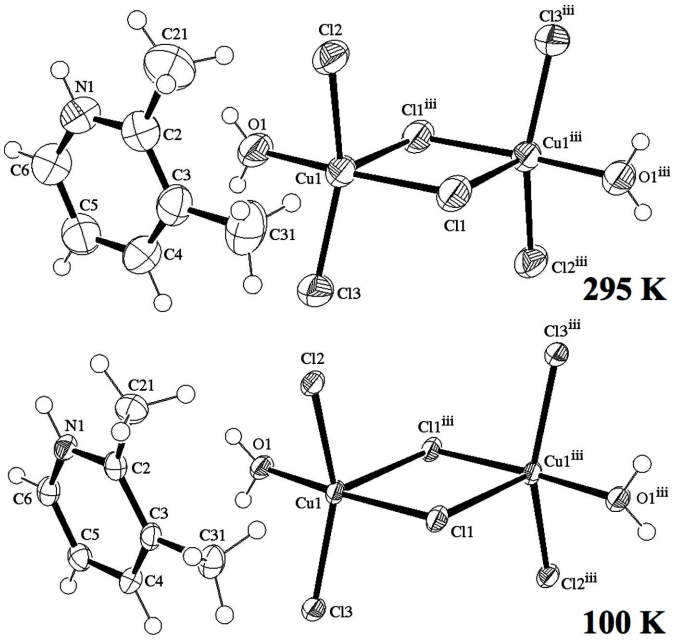

Figure 3
Views of the organic cation and $\{[CuCl_3(H_2O)]_2\}^{2-}$ dimer in (III), at 295 K (top) and 100 K (bottom), showing the atom-labeling scheme. Displacement ellipsoids are drawn at the 50% probability level. [Symmetry code: (iii) $-x+1, -y+2, -z$.]

than the 143.6 (1)° angle found in $[Cr(NH_3)_6]CuCl_5$. Since the trigonal–bipyramidal geometry of Cu^{II} is axially compressed, it is expected that the axial Cu1—Cl1 bond should be shorter than the equatorial Cu—Cl bonds. This is marginally true for (I) and (II) and partially true for (III). However, as Cl1 is also the bridging ligand, some bond lengthening due to this is to be expected. Interior Cl1—Cu1···Cl1^{ii} angles [Cl1—Cu1···Cl1^{iii} for (III)] less than 90° (ranging from 82–88°) and bridging Cu1—Cl1···Cu1^{ii} angles [Cu1—Cl1···Cu1^{iii} for (III)] greater than 90° (ranging from 92–98°) arise from stretching of the dimer as a result of mutual repulsion of the Cu^{II} ions. Displacement ellipsoid plots of (I) at 100 and 295 K are presented in Fig. 1, of (II) at 100 and 295 K in Fig. 2, and of (III) at 100 and 295 K in Fig. 3. The corresponding bond lengths and angles in the inorganic complexes are presented in Tables 2–7, respectively.

The semicoordinate bond is substantially longer at 295 K than at 100 K. This effect is most dramatic for (I), in which Cu1···Cl^{ii} lengthens from 2.7987 (8) to 2.963 (2) Å, representing an increase of 5.8%. As a result, the two complexes that constitute the dimeric unit become less closely associated at higher temperature, as indicated by the increase in the Cu1···Cu1^{ii} distance from 3.7460 (6) to 3.9313 (13) Å. Since the Cu···Cu line of the dimer is most closely aligned with *a* (and almost perpendicular to *b*), this would account for the large expansion (relative to *b*) of this axis upon heating. Similar lengthening of the semicoordinate bond at 295 K is observed for (II) and (III), although with increases of only 2.85 and 3.40%, respectively, in these cases. This would also account for the smaller increase in *a* [*a*′ for (III)] upon heating. Concomitant with the lengthening of the semicoordinate bond

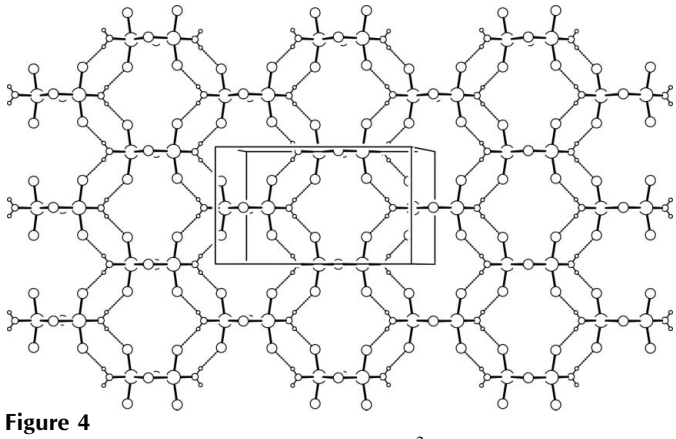

Figure 4
A packing diagram for the $\{[CuCl_3(H_2O)]_2\}^{2-}$ layer structure in the *ab* plane for (I) at 100 K, with *a* horizontal, *b* vertical and *c* out of the plane of the paper. Atoms are represented as circles of decreasing size, with Cu being the largest, then Cl, O and H. The diagram is representative of the $\{[CuCl_3(H_2O)]_2\}^{2-}$ layer structures at 100 and 295 K for (I)–(III). Hydrogen bonds are shown as dashed lines.

are slight decreases in the coordinate Cu—Cl lengths, possibly one factor in the slight contraction of *b* [*b*′ for (III)] on going from 100 to 295 K. The *trans* Cl—Cu—Cl angle increases at the higher temperature as the semicoordinate Cu···Cl bond lengthens and the complex becomes less five-coordinate, in agreement with earlier observations (Blanchette & Willett, 1988).

Each of the coordinated water ligands in the anionic dimer forms hydrogen bonds to atom Cl2 in four neighboring dimers which, in turn, form hydrogen bonds *via* their coordinated water molecules to atom Cl2 in the original dimer, to establish the two-dimensional checkerboard network in the *ab* plane shown in the packing diagram for (I) at 100 K (Fig. 4). The dimers are located on the inversion centers halfway along *a*

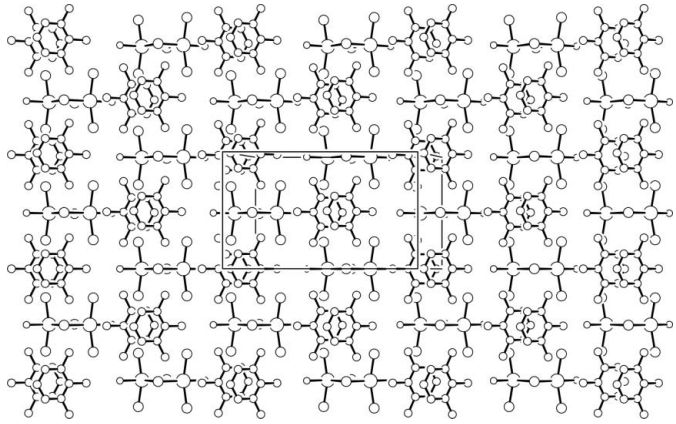

Figure 5
A packing diagram showing the placement of inversion-related 1,2,3-trimethylpyridinium cation pairs in the voids between $\{[CuCl_3(H_2O)]_2\}^{2-}$ complexes in their layer structure in the *ab* plane for (I) at 100 K, with *a* horizontal, *b* vertical and *c* out of the plane of the paper. Atoms are represented as circles of decreasing size, with Cu being the largest, then Cl, C and N, and O. H atoms have been omitted for clarity. The diagram is representative of the placement of the organic cation pairs in $\{[CuCl_3(H_2O)]_2\}^{2-}$ layer structures at 100 and 295 K for (I)–(III). The organic cation exhibits mirror-plane-generated twofold disorder in (I) and (II).

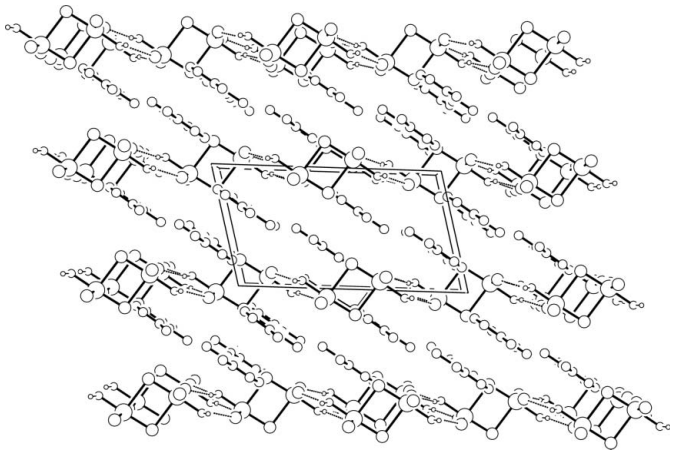

Figure 6
A packing diagram showing the alternate stacking of inorganic and organic layers along *c* (vertical, with *a* horizontal and *b* out of the plane of the paper) for (I) at 100 K. Atoms are represented as circles of decreasing size, with Cu being the largest, then Cl, C and N, and O. H atoms have been omitted for clarity. The diagram is representative of the layer stacking at 100 and 295 K for (I)–(III). The organic cation exhibits mirror-plane-generated twofold disorder in (I) and (II).

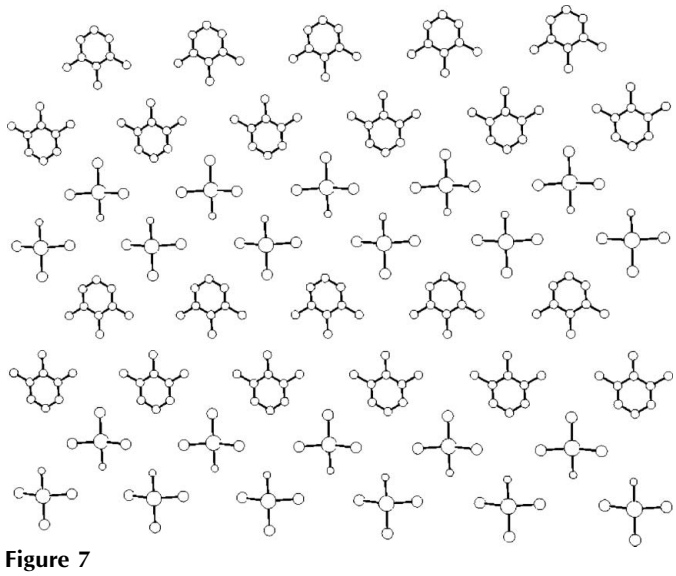

Figure 7
A packing diagram for the hybrid inorganic–organic layer in the (202) plane for (I) at 100 K, with isolated hydrate and hydrophobic columns parallel to *b* (horizontal in the diagram). Atoms are represented as circles of decreasing size, with Cu being the largest, then Cl, C and N, and O. H atoms have been omitted for clarity. The diagram is representative of the hybrid layers at 100 and 295 K for (I)–(III), with the layer plane corresponding to $(11\bar{2})$ in (III). The organic cation exhibits mirror-plane-generated twofold disorder in (I) and (II).

and *b* [only along *a* for (III)], leaving voids at the inversion centers on the corners formed by *a* and *b* and in the center of the *ab* face [or halfway along *b* for (III)]. These voids are filled above and below the anionic dimer layer by inversion-related organic cation pairs, as shown in Fig. 5 for (I) at 100 K. The alternate stacking of the inorganic network layers and organic cation-pair layers along *c* completes the three-dimensional structure of (I) at 100 K (Fig. 6).

The full symmetry of the organic cation pairs in (I) and (II) is 2/*m*, with the mirror plane 'vertical', *i.e.* perpendicular to the cation plane. Since neither the 1,2,3-trimethylpyridinium nor the 3,4-dimethylpyridinium cation possesses this symmetry, an arrangement is required whereby the ring N atom is disordered across the mirror plane, while the methyl group in the *para*-position of the ring is similarly disordered in (II). Although the 2,3-dimethylpyridinium cation in (III) does not possess vertical mirror-plane symmetry either, the ordered cation here correlates to the lower-symmetry space group. Nevertheless, the inorganic layer network structure of (I) and (II) persists without dramatic changes in (III). Given that each anionic dimer in the layer is held in place by eight different hydrogen bonds, it is not surprising that this network layer structure is robust enough to occur across significantly different crystalline environments. Specifically, the same network structure is found with the quaternary pyridinium cation in (I) as for the hydrogen-bonding cations of (II) and (III) [hydrogen-bond lengths and angles for (I)–(IV) at 100 and 295 K are presented in Table 10]. Thus, the consideration of particular organic cation–anion interactions in rationalizing the structure seems secondary. It would appear that these organic cations, with two or three adjacent methyl groups on the ring, simply fit well when packed into the network layer voids.

The stability of the network structure is further indicated by the formation of these compounds regardless of the starting stoichiometric ratio of organic cation to copper(II) chloride in solution. Our experience working with crystals of (I)–(III) raises some interesting questions regarding the relative stability of these crystalline compounds, to which we can give some tentative answers. We have, to date, identified crystals of (I) as the only product formed from acidic aqueous solution across a range (from 2:1 to 1:3) of starting stoichiometric ratios of 1,2,3-trimethylpyridinium chloride and $CuCl_2$. The emerald-green crystals of (I) are large, well faceted and high quality, although some care must be taken when cutting the crystals to avoid crystal damage. Emerald-green crystals of (II) and (III) form from acidic aqueous solutions across a range of stoichimetries, but a 2:1 ratio of organic cation to Cu^{2+} also yields yellow crystals of the $CuCl_4^{2-}$ salts, which we have structurally characterized (Nalla & Bond, 2010). The crystal quality of (II) is generally lower than for (I), with smaller and (often) poorly diffracting crystals, although high-quality crystals for X-ray studies are obtained with some patience. The crystal quality of (III), on the other hand, is execrable: small poorly faceted crystals, fused into clumps that make finding a sample suitable for X-ray studies seem, at times, a hopeless task [and to which the higher *R* value at 100 K for (III) compared with (I) and (II) attests]. Based on these observations, three adjacent methyl groups on the ring provide a more stable crystalline structure than two adjacent methyl groups. Furthermore, 2/*m* symmetry for the inorganic network is more stable than the $\bar{1}$ symmetry of (III), even with an ordered organic cation.

Do other pyridinium cations with two or three adjacent methyl groups yield the same network structure? Chloridocuprate(II) salts formed with the 1,2-dimethylpyridinium

cation have been studied, but the only compounds reported so far are the $[Cu_2Cl_5(H_2O)]^-$ (Bond & Willett, 1989) and $[Cu_6Cl_{14}]^{2-}$ salts (Bond *et al.*, 1995). It would appear that, for dimethylpyridinium cations, the presence of N—H hydrogen bonding partially compensates for the reduction in stability that occurs with one less methyl group. Since 1,2-dimethylpyridinium is incapable of N—H hydrogen bonding, that stabilizing factor is lost and other compounds are formed. To the best of our knowledge, preparation of chloridocuprate(II) salts with 2,3,4- and 3,4,5-trimethylpyridinium has not been attempted. Exploration of the crystal chemistry of these systems is attractive in order to study further the effect of three neighboring methyl groups on the chloridocuprate(II) structure, but is impeded by our difficulty in obtaining the free pyridines. The remaining cation in this class is 1,2,6-trimethylpyridinium, which would seem to be perfectly suited for this structure type. It has the same shape as 1,2,3-trimethylpyridinium, but also has vertical mirror-plane symmetry, so it should be ordered in the ideal *C*2/*m* network layer structure. Our attempts to prepare 1,2,6-trimethylpyridinium chloridocuprate(II) salts from acidic aqueous solution have so far yielded, from the range of 2:1 to 1:2 starting stoichiometries, only dark-green crystals of the $CuCl_4^{2-}$ salt (Bond *et al.*, 2005), which coincidentally also crystallizes in the monoclinic space group *C*2/*m*. This presents the interesting possibility that organic cation disorder itself may play a role in stabilizing the 2/*m* symmetry network layer structure.

Both the $[CuCl_3(H_2O)]^-$ complex and the organic cation are tilted relative to the dimer layer plane and are approximately coplanar with one another, to establish a hybrid inorganic–organic layer motif coincident with the (202) lattice plane [$(11\bar{2})$ for (III)]. A packing diagram of this hybrid layer is shown in Fig. 7 for (I) at 100 K. Within this layer, the water molecules are lined along half of the 2_1 axes of the unit cell for (I) and (II) [or parallel to b' for (III)] to form hydrate columns, while the methyl groups of the organic cations meet along the other half of the 2_1 axes of the unit cell in (I) or (II) [or parallel to b' in (III)] to form parallel hydrophobic columns. Crystals of (I), (II) and (III) are air-stable indefinitely, so there is likely little, if any, mobility into or out of these columns. In the 1,2,3-trimethylpyridinium salt, the central methyl group of the aromatic ring is directed into (and perpendicular to) the hydrophobic column, with the two neighboring methyl groups flanking it. Loss of a methyl group upon replacing trimethylpyridinium with dimethylpyridinium leads to a reduction in the packing efficiency and the lower stability of (II) and (III) relative to (I). A small decrease in molecular volume (~11 Å^3) is found for (II) and (III) compared with (I), but this is not enough to account for the volume of a lost methyl group. Assuming van der Waals radii of 2.0 Å for $-CH_3$ and 1.2 Å for H (Pauling, 1960), and assuming spherical shapes, an approximate molecular volume difference of 26 Å^3 is calculated for replacement of a ring methyl group by hydrogen. This corresponds well to the difference in molecular volume of ~25 Å^3 between the structures of 3,4-dimethylpyridinium bromide (CSD refcode NUNDIJ, 157 K; Bolte & Kettner, 1998) and 4-methyl- (WABYUT, ambient temperature; Andras *et al.*, 1993) or 3-methylpyridinium bromide (DICJEE, 173 K; Faber *et al.*, 1999). Thus, the molecular volumes for (II) and (III) are ~15 Å^3 larger than expected. A calculation of voids (*Mercury*, Version 2.4; Macrae *et al.*, 2008) within the unit cell for (III) at 100 K finds the largest voids at the *para*-position of the aromatic rings [and at the site of the third methyl group in (I)], with a volume of 13.6 Å^3 for each void (probe radius = 0.9 Å, grid spacing = 0.1 Å). By comparison, a similar calculation for (I) at 100 K yields no voids at this probe radius.

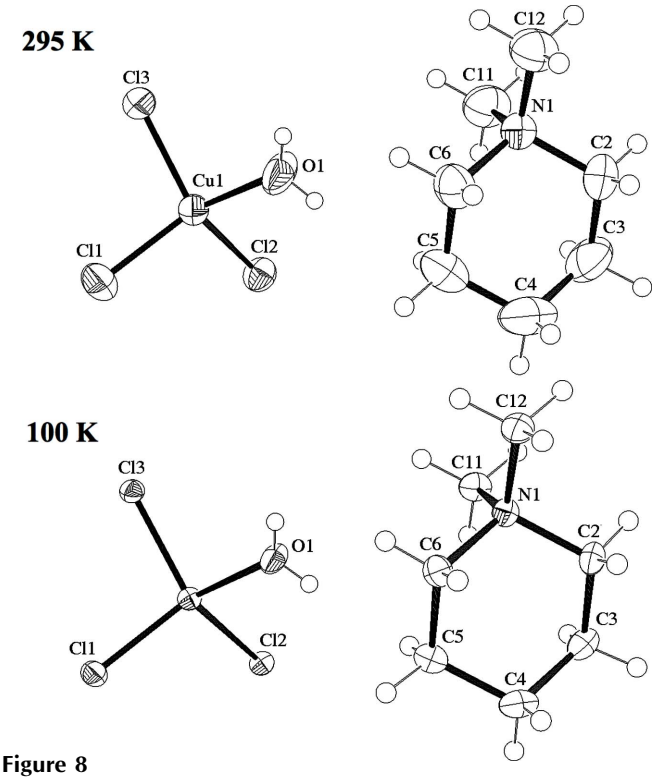

Figure 8
Views of the organic cation and $[CuCl_3(H_2O)]^-$ complex in (IV), at 295 K (top) and 100 K (bottom), showing the atom-labeling scheme. Displacement ellipsoids are drawn at the 50% probability level.

The 1,1-dimethylpiperidinium salt, (IV), has a quite different structure compared with (I)–(III). The organic cation bears some similarity to the 1,4-dimethylpiperazinium cation of KESYOW (Valle & Ettorre, 1992). However, with only one N atom, 1,1-dimethylpiperidinium is a monocation and has both methyl groups on the same atom, instead of on opposite sides of the ring. Thus, the bulkier cation in (IV), and the higher ratio of organic cation to Cu^{II}, prevent aggregation of the complexes into the semicoordinate bonded stacks found in KESYOW. This results in the flattened tetrahedral geometry expected for an isolated $[CuCl_3(H_2O)]^-$ complex, in which the *trans* Cl—Cu—Cl or —(OH_2) angles are in the range 140–142°, rather than almost 180° in KESYOW. The Cu1—Cl1 bond (*trans* to O1) is slightly shorter (2.20–2.21 Å) than the other two Cu—Cl bonds (2.22–2.24 Å). However, the latter two Cl atoms are involved in hydrogen bonding with aqua ligands on neighboring complexes, while Cl1 is not. There is little change in geometric parameters between the 100 and 295 K structures, except for a slight shortening of the Cu—O

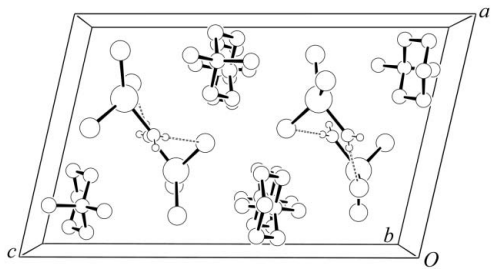

Figure 9
A packing diagram for (IV), viewed down the *b* axis, with *a* vertical and *c* horizontal, showing the hydrate columns along the 2_1 screw axes. Atoms are represented as circles of decreasing size, with Cu being the largest, then Cl, C and N, O and aqua H. H atoms bound to carbon have been omitted for clarity. Hydrogen bonds are shown as dashed lines.

bond and, likewise, a slight lengthening of the Cu—Cl bonds. Displacement ellipsoid plots of the asymmetric unit of (IV) at 100 and 295 K are presented in Fig. 8, while bond lengths and angles in the inorganic complex are presented in Tables 8 and 9 for the 100 and 295 K structures, respectively.

The $[CuCl_3(H_2O)]^-$ complexes in (IV) are aggregated into stacks, in which neighboring complexes are connected through hydrogen bonding between the aqua ligand and chloride ions of neighboring complexes in a side-to-side manner, as shown in the packing diagram at 100 K (Fig. 9), rather than the face-to-face manner in which the semicoordinated quasiplanar $[CuCl_3(H_2O)]^-$ complexes of KESYOW stack. Neighboring complexes in the stack are related by a 2_1 screw axis, with the aqua ligands concentrated in the center of the stack (and along one-half of the screw axes of the crystal). The $[CuCl_3(H_2O)]^-$ complexes are directed away from the center of the stack to generate a zigzag pattern. Stacks of complexes are separated from one another by parallel stacks of translationally equivalent organic cations. The organic cations are oriented with their long axes almost parallel to *b*, to align closely with the orientation of the long axes of the inorganic complexes. The displacement ellipsoid of the aqua O atom is significantly elongated and tilted away from the stacking axis in both the 100 and 295 K structures, which might indicate mobility of the water molecules in these columns. Indeed, crystals of (IV) are not stable to air and convert to red–brown solids of poor crystallinity over a period of 2–3 weeks. Manfredini *et al.* (1990) noted a similar color change on dehydration of KESYOW and KESYUC, and this is likely the source of the color change here.

Experimental

For quaternary pyridinium or piperidinium salts, 2,3-dimethylpyridine (5 ml) or 1-methylpiperidine (5 ml) was reacted with excess iodomethane. The resulting iodide salt was converted into the chloride salt by reaction with excess AgCl in aqueous solution. Otherwise, dimethylpyridine (5 ml) was neutralized with excess concentrated HCl. The organic cation halide and copper(II) chloride dihydrate were combined in a 1:1 molar ratio in a solution made 6 *M* in HCl. Emerald-green crystals of (I), (II) and (III), and light-green crystals of (IV), were obtained upon evaporation.

Compound (I) at 100 K

Crystal data

$(C_8H_{12}N)[CuCl_3(H_2O)]$
M_r = 310.09
Monoclinic, $C2/m$
a = 15.4606 (4) Å
b = 9.2495 (3) Å
c = 8.4159 (2) Å
β = 104.270 (2)°
V = 1166.36 (6) Å^3
Z = 4
Mo $K\alpha$ radiation
μ = 2.53 mm^{-1}
T = 100 K
0.25 × 0.17 × 0.09 mm

Data collection

Nonius KappaCCD area-detector diffractometer
Absorption correction: multi-scan (*DENZO/SCALEPACK*; Otwinowski & Minor, 1997)
T_{min} = 0.610, T_{max} = 0.704
3004 measured reflections
1593 independent reflections
1457 reflections with $I > 2\sigma(I)$
R_{int} = 0.015

Refinement

$R[F^2 > 2\sigma(F^2)]$ = 0.027
$wR(F^2)$ = 0.067
S = 1.13
1593 reflections
79 parameters
1 restraint
H atoms treated by a mixture of independent and constrained refinement
$\Delta\rho_{max}$ = 0.58 e Å^{-3}
$\Delta\rho_{min}$ = −0.56 e Å^{-3}

Compound (I) at 295 K

Crystal data

$(C_8H_{12}N)[CuCl_3(H_2O)]$
M_r = 310.09
Monoclinic, $C2/m$
a = 15.6883 (19) Å
b = 9.2405 (10) Å
c = 8.5073 (10) Å
β = 103.521 (9)°
V = 1199.1 (2) Å^3
Z = 4
Mo $K\alpha$ radiation
μ = 2.46 mm^{-1}
T = 295 K
0.30 × 0.13 × 0.08 mm

Data collection

Nonius KappaCCD area-detector diffractometer
Absorption correction: multi-scan (*DENZO/SCALEPACK*; Otwinowski & Minor, 1997)
T_{min} = 0.631, T_{max} = 0.875
2595 measured reflections
1440 independent reflections
1184 reflections with $I > 2\sigma(I)$
R_{int} = 0.023

Refinement

$R[F^2 > 2\sigma(F^2)]$ = 0.042
$wR(F^2)$ = 0.112
S = 1.09
1440 reflections
79 parameters
1 restraint
H atoms treated by a mixture of independent and constrained refinement
$\Delta\rho_{max}$ = 1.24 e Å^{-3}
$\Delta\rho_{min}$ = −0.97 e Å^{-3}

Compound (II) at 100 K

Crystal data

$(C_7H_{10}N)[CuCl_3(H_2O)]$
M_r = 296.07
Monoclinic, $C2/m$
a = 15.1429 (4) Å
b = 8.8854 (2) Å
c = 8.5918 (2) Å
β = 104.262 (2)°
V = 1120.40 (5) Å^3
Z = 4
Mo $K\alpha$ radiation
μ = 2.63 mm^{-1}
T = 100 K
0.17 × 0.08 × 0.05 mm

Table 1
Known geometries and aggregation motifs for $[CuCl_3(H_2O)]^-$ complexes.

Counter-ion	CSD refcode	Geometry	Aggregation motif
Salicylideneguanylhydrazinium[a]	GEMJIS	*mm*2 distorted trigonal–bipyramidal	Monobridged and hydrogen-bonded chains
1,4-Dimethylpiperazinium[b]	KESYOW	Planar	$1(\frac{1}{2}, \frac{1}{2}, 180^\circ)(-\frac{1}{2}, -\frac{1}{2}, 180^\circ)$ dibridged stacks
2-Aminopyrimidinium[b]	KESYUC	Planar	$1(\frac{1}{2}, \frac{1}{2})$ dibridged stacks
Chloroimidazolium[c]	KOTDOM	Planar	$1(\frac{1}{2}, \frac{1}{2}, 180^\circ)$ dibridged stacks
Bis{[2-(*N*,*N*-dipicolylamino)acylglycine ethyl ester]chlorocopper(II)}[d]	QOMTUH	Tetrahedral	Isolated
Hexaoxa-1,10-diazoniabicyclo[8.8.8]-hexacosane[e]	REGVOP	Flattened tetrahedral	Chains of hydrogen-bonded dimers monobridged to $[CuCl_4]^{2-}$
Dibenzyl-4,4′-bipyridinium[f]	VITSAS	Flattened tetrahedral	Ribbons from monobridging to $[CuCl_4]^{2-}$ and $[CuCl_2]^-$
4,5-Diazoniafluoren-9-one[g]	WETFAC	*mm*2 distorted trigonal–bipyramidal	Herringbone ribbons from hydrogen and coordinate bonds to lattice Cl
1,3-Xylylenediammonium[h]	XISPAQ	Planar	$1(\frac{1}{2}, \frac{1}{2}, 180^\circ)(-\frac{1}{2}, -\frac{1}{2}, 180^\circ)$ dibridged stacks
2-Chlorido- or 2-bromido-2-imidazolinium[i]	HEPQUA, HEPQUA01 for 2-bromido	Planar	$1(\frac{1}{2}, \frac{1}{2}, 180^\circ)$ stacks
1,2,3-Trimethyl-, 2,3- or 3,4-dimethyl-pyridinium[j]		*mm*2 distorted trigonal–bipyramidal	Hydrogen-bonded network of dibridged dimers
N,*N*-Dimethylpiperidinium[j]		Flattened tetrahedral	Hydrogen-bonded chains

References: (*a*) Chumakov *et al.* (2006); (*b*) Manfredini *et al.* (1990); (*c*) Valle & Ettorre (1992); (*d*) Niklas *et al.* (2001); (*e*) Chekhlov (2005); (*f*) Scott & Willett (1991); (*g*) Menon *et al.* (1994); (*h*) Haddad *et al.* (2001); (*i*) Diaz *et al.* (1998); (*j*) this work.

Data collection

Nonius KappaCCD area-detector diffractometer
Absorption correction: multi-scan (*DENZO*/*SCALEPACK*; Otwinowski & Minor, 1997)
T_{min} = 0.716, T_{max} = 0.884
3544 measured reflections
1880 independent reflections
1663 reflections with $I > 2\sigma(I)$
R_{int} = 0.017

Refinement

$R[F^2 > 2\sigma(F^2)]$ = 0.026
$wR(F^2)$ = 0.062
S = 1.08
1880 reflections
77 parameters
H atoms treated by a mixture of independent and constrained refinement
$\Delta\rho_{max}$ = 0.59 e Å^{-3}
$\Delta\rho_{min}$ = −0.80 e Å^{-3}

Table 2
Selected geometric parameters (Å, °) for (I) at 100 K.

Cu1—Cl1	2.2547 (7)	Cu1—Cl2	2.2848 (5)
Cu1—Cl1^{ii}	2.7988 (8)	Cu1—O1	1.995 (2)
Cl1—Cu1—Cl1^{ii}	84.93 (2)	Cl1—Cu1—O1	177.73 (7)
Cl1—Cu1—Cl2	93.044 (14)	Cl1^{ii}—Cu1—O1	92.80 (7)
Cl1^{ii}—Cu1—Cl2	101.961 (14)	Cl2—Cu1—O1	87.421 (19)
Cl2—Cu1—Cl2^{i}	155.74 (3)	Cu1—Cl1—Cu1^{ii}	95.07 (2)

Symmetry codes: (i) $x, -y, z$; (ii) $-x+1, y, -z$.

Table 3
Selected geometric parameters (Å, °) for (I) at 295 K.

Cu1—Cl1	2.2428 (14)	Cu1—Cl2	2.2750 (9)
Cu1—Cl1^{ii}	2.964 (2)	Cu1—O1	1.999 (4)
Cl1—Cu1—Cl1^{ii}	82.91 (6)	Cl1—Cu1—O1	175.81 (15)
Cl1—Cu1—Cl2	93.60 (3)	Cl1^{ii}—Cu1—O1	92.90 (17)
Cl1^{ii}—Cu1—Cl2	100.71 (3)	Cl2—Cu1—O1	87.16 (4)
Cl2—Cu1—Cl2^{i}	158.09 (6)	Cu1—Cl1—Cu1^{ii}	97.09 (6)

Symmetry codes: (i) $x, -y, z$; (ii) $-x+1, y, -z$.

Compound (II) at 295 K

Crystal data

$(C_7H_{10}N)[CuCl_3(H_2O)]$
M_r = 296.07
Monoclinic, $C2/m$
a = 15.3144 (4) Å
b = 8.8708 (2) Å
c = 8.7761 (2) Å
β = 103.967 (2)°
V = 1156.99 (5) Å^3
Z = 4
Mo $K\alpha$ radiation
μ = 2.54 mm^{-1}
T = 295 K
0.17 × 0.08 × 0.05 mm

Data collection

Nonius KappaCCD area-detector diffractometer
Absorption correction: multi-scan (*DENZO*/*SCALEPACK*; Otwinowski & Minor, 1997)
T_{min} = 0.727, T_{max} = 0.880
3244 measured reflections
1724 independent reflections
1485 reflections with $I > 2\sigma(I)$
R_{int} = 0.013

Table 4
Selected geometric parameters (Å, °) for (II) at 100 K.

Cu1—Cl1	2.2708 (5)	Cu1—Cl2	2.2742 (3)
Cu1—Cl1^{ii}	2.7632 (6)	Cu1—O1	1.9747 (16)
Cl1—Cu1—Cl1^{ii}	87.684 (18)	Cl1—Cu1—O1	175.44 (6)
Cl1—Cu1—Cl2	92.453 (11)	Cl1^{ii}—Cu1—O1	87.76 (6)
Cl1^{ii}—Cu1—Cl2	101.920 (12)	Cl2—Cu1—O1	88.489 (15)
Cl2—Cu1—Cl2^{i}	155.83 (2)	Cu1—Cl1—Cu1^{ii}	92.316 (18)

Symmetry codes: (i) $x, -y, z$; (ii) $-x+1, y, -z$.

Table 5
Selected geometric parameters (Å, °) for (II) at 295 K.

Cu1—Cl1	2.2642 (8)	Cu1—Cl2	2.2694 (5)
Cu1—Cl1^{ii}	2.8412 (11)	Cu1—O1	1.980 (2)
Cl1—Cu1—Cl1^{ii}	86.43 (3)	Cl1—Cu1—O1	174.23 (11)
Cl1—Cu1—Cl2	93.006 (17)	Cl1^{ii}—Cu1—O1	87.80 (11)
Cl1^{ii}—Cu1—Cl2	101.25 (2)	Cl2—Cu1—O1	88.12 (3)
Cl2—Cu1—Cl2^{i}	157.01 (4)	Cu1—Cl1—Cu1^{ii}	93.57 (3)

Symmetry codes: (i) $x, -y, z$; (ii) $-x+1, y, -z$.

Refinement

$R[F^2 > 2\sigma(F^2)] = 0.033$
$wR(F^2) = 0.090$
$S = 1.06$
1724 reflections
77 parameters
2 restraints

H atoms treated by a mixture of independent and constrained refinement
$\Delta\rho_{max} = 0.71$ e Å^{-3}
$\Delta\rho_{min} = -0.57$ e Å^{-3}

Compound (III) at 100 K

Crystal data

$(C_7H_{10}N)[CuCl_3(H_2O)]$
$M_r = 296.07$
Triclinic, $P\overline{1}$
$a = 8.8088$ (4) Å
$b = 8.7803$ (4) Å
$c = 8.7570$ (4) Å
$\alpha = 74.101$ (3)°
$\beta = 76.513$ (4)°
$\gamma = 59.895$ (7)°
$V = 559.77$ (6) Å^3
$Z = 2$
Mo $K\alpha$ radiation
$\mu = 2.63$ mm^{-1}
$T = 100$ K
0.23 × 0.12 × 0.08 mm

Data collection

Nonius KappaCCD area-detector diffractometer
Absorption correction: multi-scan (*DENZO*/*SCALEPACK*; Otwinowski & Minor, 1997)
$T_{min} = 0.589$, $T_{max} = 0.826$
4879 measured reflections
2554 independent reflections
2349 reflections with $I > 2\sigma(I)$
$R_{int} = 0.024$

Refinement

$R[F^2 > 2\sigma(F^2)] = 0.046$
$wR(F^2) = 0.124$
$S = 1.16$
2554 reflections
129 parameters
2 restraints

H atoms treated by a mixture of independent and constrained refinement
$\Delta\rho_{max} = 1.13$ e Å^{-3}
$\Delta\rho_{min} = -0.76$ e Å^{-3}

Compound (III) at 295 K

Crystal data

$(C_7H_{10}N)[CuCl_3(H_2O)]$
$M_r = 296.07$
Triclinic, $P\overline{1}$
$a = 8.8369$ (4) Å
$b = 8.8282$ (4) Å
$c = 8.9410$ (4) Å
$\alpha = 74.628$ (3)°
$\beta = 77.056$ (4)°
$\gamma = 59.517$ (7)°
$V = 576.23$ (5) Å^3
$Z = 2$
Mo $K\alpha$ radiation
$\mu = 2.55$ mm^{-1}
$T = 295$ K
0.23 × 0.12 × 0.08 mm

Data collection

Nonius KappaCCD area-detector diffractometer
Absorption correction: multi-scan (*DENZO*/*SCALEPACK*; Otwinowski & Minor, 1997)
$T_{min} = 0.607$, $T_{max} = 0.823$
4951 measured reflections
2586 independent reflections
2179 reflections with $I > 2\sigma(I)$
$R_{int} = 0.025$

Refinement

$R[F^2 > 2\sigma(F^2)] = 0.044$
$wR(F^2) = 0.128$
$S = 1.13$
2584 reflections
130 parameters
2 restraints

H atoms treated by a mixture of independent and constrained refinement
$\Delta\rho_{max} = 1.06$ e Å^{-3}
$\Delta\rho_{min} = -0.49$ e Å^{-3}

Table 6
Selected geometric parameters (Å, °) for (III) at 100 K.

Cu1—Cl1	2.2705 (11)	Cu1—Cl3	2.2644 (11)
Cu1—Cl1^{iii}	2.7928 (12)	Cu1—O1	1.978 (3)
Cu1—Cl2	2.2790 (11)		
Cl1—Cu1—Cl1^{iii}	85.90 (4)	Cl1—Cu1—O1	172.77 (10)
Cl1—Cu1—Cl2	92.68 (4)	Cl1^{iii}—Cu1—O1	86.87 (10)
Cl1^{iii}—Cu1—Cl2	101.15 (4)	Cl2—Cu1—O1	88.97 (10)
Cl1—Cu1—Cl3	92.99 (4)	Cl3—Cu1—O1	88.72 (10)
Cl1^{iii}—Cu1—Cl3	105.74 (4)	Cu1—Cl1—Cu1^{iii}	94.10 (4)
Cl2—Cu1—Cl3	152.84 (5)		

Symmetry code: (iii) $-x+1, -y+2, -z$.

Table 7
Selected geometric parameters (Å, °) for (III) at 295 K.

Cu1—Cl1	2.2617 (10)	Cu1—Cl3	2.2601 (11)
Cu1—Cl1^{iii}	2.8910 (13)	Cu1—O1	1.976 (3)
Cu1—Cl2	2.2683 (10)		
Cl1—Cu1—Cl1^{iii}	85.20 (4)	Cl1^{iii}—Cu1—O1	86.43 (13)
Cl1—Cu1—Cl2	93.06 (4)	Cl2—Cu1—O1	88.78 (10)
Cl1^{iii}—Cu1—Cl2	100.49 (4)	Cl2—Cu1—Cl3	154.30 (5)
Cl1—Cu1—Cl3	93.37 (4)	Cl3—Cu1—O1	88.45 (10)
Cl1^{iii}—Cu1—Cl3	104.83 (4)	Cu1—Cl1—Cu1^{iii}	94.80 (4)
Cl1—Cu1—O1	171.62 (11)		

Symmetry code: (iii) $-x+1, -y+2, -z$.

Compound (IV) at 100 K

Crystal data

$(C_7H_{16}N)[CuCl_3(H_2O)]$
$M_r = 302.11$
Monoclinic, $P2_1/c$
$a = 10.1958$ (3) Å
$b = 7.6080$ (3) Å
$c = 16.3281$ (5) Å
$\beta = 102.927$ (2)°
$V = 1234.46$ (7) Å^3
$Z = 4$
Mo $K\alpha$ radiation
$\mu = 2.38$ mm^{-1}
$T = 100$ K
0.37 × 0.13 × 0.07 mm

Data collection

Nonius KappaCCD area-detector diffractometer
Absorption correction: multi-scan (*DENZO*/*SCALEPACK*; Otwinowski & Minor, 1997)
$T_{min} = 0.665$, $T_{max} = 0.771$
6071 measured reflections
3187 independent reflections
2587 reflections with $I > 2\sigma(I)$
$R_{int} = 0.032$

Refinement

$R[F^2 > 2\sigma(F^2)] = 0.036$
$wR(F^2) = 0.081$
$S = 1.10$
3187 reflections
129 parameters

H atoms treated by a mixture of independent and constrained refinement
$\Delta\rho_{max} = 0.63$ e Å^{-3}
$\Delta\rho_{min} = -0.75$ e Å^{-3}

Compound (IV) at 295 K

Crystal data

$(C_7H_{16}N)[CuCl_3(H_2O)]$
$M_r = 302.11$
Monoclinic, $P2_1/c$
$a = 10.3459$ (2) Å
$b = 7.6409$ (2) Å
$c = 16.5616$ (4) Å
$\beta = 103.746$ (2)°
$V = 1271.73$ (5) Å^3
$Z = 4$
Mo $K\alpha$ radiation
$\mu = 2.31$ mm^{-1}
$T = 295$ K
0.37 × 0.13 × 0.07 mm

Table 8
Selected geometric parameters (Å, °) for (IV) at 100 K.

Cu1—Cl1	2.2089 (7)	Cu1—Cl3	2.2391 (7)
Cu1—Cl2	2.2315 (7)	Cu1—O1	1.971 (2)
Cl1—Cu1—Cl2	100.47 (3)	Cl2—Cu1—Cl3	140.44 (3)
Cl1—Cu1—Cl3	100.45 (3)	Cl2—Cu1—O1	91.53 (7)
Cl1—Cu1—O1	141.42 (8)	Cl3—Cu1—O1	92.62 (8)

Table 9
Selected geometric parameters (Å, °) for (IV) at 295 K.

Cu1—Cl1	2.2030 (7)	Cu1—Cl3	2.2342 (7)
Cu1—Cl2	2.2263 (7)	Cu1—O1	1.981 (2)
Cl1—Cu1—Cl2	100.52 (3)	Cl1—Cu1—O1	140.10 (10)
Cl1—Cu1—Cl3	100.51 (3)	Cl2—Cu1—O1	91.68 (7)
Cl2—Cu1—Cl3	141.20 (3)	Cl3—Cu1—O1	92.69 (7)

Table 10
Hydrogen-bond geometry (Å, °) for (I)–(IV) at 100 and 295 K.

Compound and temperature	D—H···A	D—H	H···A	D···A	D—H···A
(I), 100 K	O1—H1···Cl2^{v}	0.812 (10)	2.46 (3)	3.242 (2)	163 (2)
(I), 295 K	O1—H1···Cl2^{v}	0.817 (10)	2.48 (5)	3.252 (4)	157 (4)
(II), 100 K	O1—H1*W*···Cl2^{v}	0.74 (2)	2.45 (2)	3.153 (1)	160 (2)
(II), 100 K	N1—H1···Cl1^{vi}	0.86	2.448 (1)	3.274 (4)	161.1 (3)
(II), 295 K	O1—H1*W*···Cl2^{v}	0.812 (9)	2.402 (19)	3.171 (2)	158.4 (6)
(II), 295 K	N1*A*—H1*A*···Cl1^{vii}	0.86	2.588	3.418	163
(III), 100 K	O1—H1*WA*···Cl3^{viii}	0.818 (10)	2.38 (5)	3.154 (4)	159 (2)
(III), 100 K	O1—H1*WB*···Cl2^{ix}	0.820 (10)	2.34 (5)	3.129 (4)	161 (5)
(III), 100 K	N1—H1···Cl1^{x}	0.86	2.358	3.209	170
(III), 295 K	O1—H1*WA*···Cl3^{viii}	0.818 (10)	2.42 (6)	3.168 (4)	153 (3)
(III), 295 K	O1—H1*WB*···Cl2^{ix}	0.820 (10)	2.35 (6)	3.142 (4)	163 (6)
(III), 295 K	N1—H1···Cl1^{x}	0.86	2.366	3.219	171
(IV), 100 K	O1—H1*A*···Cl2^{x}	0.75 (4)	2.32 (4)	3.065 (3)	173 (4)
(IV), 100 K	O1—H1*B*···Cl3^{xi}	0.78 (4)	2.33 (3)	3.100 (2)	171 (3)
(IV), 295 K	O1—H1*A*···Cl2^{x}	0.812 (10)	2.28 (3)	3.088 (3)	178 (3)
(IV), 295 K	O1—H1*B*···Cl3^{xi}	0.814 (10)	2.31 (3)	3.112 (2)	169 (3)

Symmetry codes: (v) $-x+\frac{3}{2}, -y+\frac{1}{2}, -z$; (vi) $x+\frac{1}{2}, y-\frac{1}{2}, z$; (vii) $x+\frac{1}{2}, y+\frac{1}{2}, z$; (viii) $-x+1, -y+1, -z$; (ix) $-x, -y+2, -z$; (x) $x-1, y, z$; (xi) $-x+1, -y-1, -z+1$.

Data collection

Nonius KappaCCD area-detector diffractometer
Absorption correction: multi-scan (*DENZO*/*SCALEPACK*; Otwinowski & Minor, 1997)
T_{min} = 0.680, T_{max} = 0.783
5547 measured reflections
2909 independent reflections
2414 reflections with $I > 2\sigma(I)$
R_{int} = 0.023

Refinement

$R[F^2 > 2\sigma(F^2)]$ = 0.032
$wR(F^2)$ = 0.083
S = 1.05
2909 reflections
128 parameters
2 restraints
H atoms treated by a mixture of independent and constrained refinement
$\Delta\rho_{max}$ = 0.45 e Å^{-3}
$\Delta\rho_{min}$ = −0.39 e Å^{-3}

H atoms were visible in difference electron-density maps but were placed geometrically and refined using a riding model, with aromatic C—H, methyl C—H, methylene C—H and aromatic N—H distances fixed at 0.93, 0.96, 0.97 and 0.86 Å, respectively. Torsion angles for methyl groups were refined to match the electron density. Aqua H atoms were refined with the O—H bond length loosely restrained to 0.82 Å, except for (II) and (IV) at 100 K, in which they were freely refined. Bond lengths and angles within organic cations conform to expected values (Ladd & Palmer, 1994). Secondary extinction corrections were refined (Alcock, 1974), except for (I) and (III) at 100 K. For the disordered stuctures of (I) and (II), solution and refinement in the noncentrosymmetric space group *C*2 did not resolve the disorder or improve agreement factors significantly. Low-angle reflections blocked by the beam catcher shadow (as shown by $F_o^2 << F_c^2$) were omitted from the refinement. Exceptions to this procedure are described below.

For (I), to describe the mirror-generated disorder, atoms N1 and C3 were each given site-occupation factors of 0.5 and required to have the same positional and displacement parameters. The methyl group at C21 was calculated to have mirror plane symmetry for the 295 K structure.

For (II), mirror-generated disorder of the organic cation was modelled in the 295 K structure with two different fragments, each with half the full site-occupation factors, so that the mirror related part of one fragment completes the other fragment and *vice versa*. Within each of the atom pairs C3/C3*A*, C31/C31*A*, C4/C2*A*, C5/N1*A* and C6/C6*A*, the same position and displacement parameters were required. Refinement of the 100 K structure with three atoms of the cation ring on the mirror plane revealed elongated ellipsoids, indicating that the ring was canted off the plane. Final refinement used a complete cation with all atoms off the mirror plane and each with a site occupancy of 0.5. Isotropic displacement parameters were refined for the aromatic ring C and N atoms due to their close proximity in the disordered arrangement. At 295 K, the methyl groups were calculated to give twofold disorder, and atoms H6/H6*A* were initially refined with tight restraints but fixed in a riding model for the final cycles of refinement.

For (III), the unit-cell constants were chosen to match the orientation of the reduced cell constants in (I) and (II).

For (IV), a common isotropic displacement parameter was refined at 295 K for the aqua H atoms.

For all determinations, data collection: *COLLECT* (Nonius, 1998); cell refinement: *SCALEPACK* (Otwinowski & Minor, 1997); data reduction: *DENZO* (Otwinowski & Minor, 1997) and *SCALEPACK*; program(s) used to solve structure: *SIR92* (Altomare *et al.*, 1993); program(s) used to refine structure: *SHELXL97* (Sheldrick, 2008); molecular graphics: *ORTEP-3 for Windows* (Farrugia, 1997); software used to prepare material for publication: *WinGX* (Farrugia, 1999).

The authors thank the National Science Foundation DUE CCLI–A&I program (grant No. 9951348) and Southeast Missouri State University for funding the X-ray diffraction facility.

Supplementary data for this paper are available from the IUCr electronic archives (Reference: BM3105). Services for accessing these data are described at the back of the journal.

References

Alcock, N. W. (1974). *Acta Cryst.* A**30**, 332–335.
Allen, F. H. (2002). *Acta Cryst.* B**58**, 380–388.
Altomare, A., Cascarano, G., Giacovazzo, C. & Guagliardi, A. (1993). *J. Appl. Cryst.* **26**, 343–350.

Andras, M. T., Hepp, A. F., Fanwick, P. E., Martuch, R. A. & Duraj, S. A. (1993). *Acta Cryst.* C**49**, 548–550.
Blanchette, J. T. & Willett, R. D. (1988). *Inorg. Chem.* **33**, 950–954.
Bolte, M. & Kettner, M. (1998). *Acta Cryst.* C**54**, 963–964.
Bond, M. R., Gerdes, A. & Kelley, A. F. (2005). *Acta Cryst.* A**61**, C301.
Bond, M. R., Place, H., Wang, Z., Willett, R. D., Liu, Y., Grigereit, T. E., Drumheller, J. E. & Tuthill, G. F. (1995). *Inorg. Chem.* **34**, 3134–3141.
Bond, M. R. & Willett, R. D. (1989). *Inorg. Chem.* **28**, 3267–3269.
Chekhlov, A. N. (2005). *Zh. Neorg. Khim.* **50**, 1656–1661.
Chumakov, Yu. M., Tsapkov, V. I., Bocelli, G., Antosyak, B. Ya., Shova, S. G. & Gulya, A. P. (2006). *Kristallografiya*, **51**, 66–74.
Diaz, I., Fernández, V., Martínez, J. L., Beyer, L., Pilz, A. & Müller, U. (1998). *Z. Naturforsch. Teil B*, **53**, 933–938.
Dobrzycki, L. & Wozniak, K. (2008). *CrystEngComm*, **10**, 525–533.
Faber, A., Lemke, A., Spangenberg, B. & Bolte, M. (1999). *Acta Cryst.* C**55**, IUC9900156.
Farrugia, L. J. (1997). *J. Appl. Cryst.* **30**, 565.
Farrugia, L. J. (1999). *J. Appl. Cryst.* **32**, 837–838.
Haddad, S. F., Willett, R. D. & Landee, C. P. (2001). *Inorg. Chim. Acta*, **316**, 94–98.
Ladd, M. F. C. & Palmer, R. A. (1994). *Structure Determination by X-ray Crystallography*, 3rd ed., pp. 434–435. New York: Plenum Press.
Macrae, C. F., Bruno, I. J., Chisholm, J. A., Edgington, P. R., McCabe, P., Pidcock, E., Rodriguez-Monge, L., Taylor, R., van de Streek, J. & Wood, P. A. (2008). *J. Appl. Cryst.* **41**, 466–470.
Manfredini, T., Pellacani, G. C., Bonamartini-Corradi, A., Battaglia, L. P., Guarini, G. G. T., Giusti, J. G., Pon, G., Willett, R. D. & West, D. X. (1990). *Inorg. Chem.* **29**, 2221–2228.
Menon, S., Balagopalakrishna, C., Rajasekharan, M. V. & Ramakrishna, B. L. (1994). *Inorg. Chem.* **33**, 950–954.
Nalla, S. & Bond, M. R. (2010). Unpublished work.
Niklas, N., Wolf, S., Liehr, G., Anson, C. E., Powell, A. K. & Alsfasser, R. (2001). *Inorg. Chim. Acta*, **314**, 126–132.
Nonius (1998). *COLLECT*. Nonius BV, Delft, The Netherlands.
Ohba, S., Fujita, T. & Bernal, I. (1995). *Acta Cryst.* C**51**, 1481–1483.
Otwinowski, Z. & Minor, W. (1997). *Methods in Enzymology*, Vol. 276, *Macromolecular Crystallography*, Part A, edited by C. W. Carter Jr & R. M. Sweet, pp. 307–326. New York: Academic Press.
Pauling, L. (1960). *The Nature of the Chemical Bond*, 3rd ed., pp. 260–261. Ithaca, NY: Cornell University Press.
Reinen, D. & Astanasov, M. (1989). *Chem. Phys.* **136**, 27–46.
Reinen, D. & Friebel, C. (1984). *Inorg. Chem.* **23**, 791–798.
Savel'eva, Z. A., Romanenko, G. V., Podberezskaya, N. V., Sheludyakova, L. A., Shvedenkov, Y. G. & Larionov, S. V. (1999). *Koord. Khim.* **25**, 370–375.
Scott, B. & Willett, R. D. (1991). *Acta Cryst.* C**47**, 1389–1392.
Sheldrick, G. M. (2008). *Acta Cryst.* A**64**, 112–122.
Valle, G. & Ettorre, R. (1992). *Acta Cryst.* C**48**, 919–921.
Willett, R. D. (1985). *Magneto-Structural Correlations in Exchange Coupled Systems*. NATO ASI Series, No. C140, edited by R. D. Willett, D. Gatteschi & O. Kahn, pp. 389–420. Dordrecht: Reidel.